Pseudo-surface acoustic wave studies on MF_2/GaAs(111) heterostructures using Brillouin scattering

1994 J. Phys.: Condens. Matter 6 3347

(http://iopscience.iop.org/0953-8984/6/18/011)

J. Phys.: Condens. Matter 6 (1994) 3347–3358. Printed in the UK

Pseudo-surface acoustic wave studies on MF_2/GaAs(111) heterostructures using Brillouin scattering

V V Aleksandrov†, M V Saphonov†, V R Velasco‡, N L Yakovlev§ and L Ph Martynenko§

† Physics Department, Moscow State University, Moscow 117 234, Russia
‡ Instituto de Ciencia de Materiales, CSIC, Serrano 123, 28 006 Madrid, Spain
§ A F Ioffe Physico-Technical Institute, Russian Academy of Science, Politeknichskaya 26, St Petersburg, Russia

Received 23 November 1993, in final form 2 February 1994

Abstract. We present here the registration of pseudo-surface modes, PSMs, propagating on MF_2/GaAs(111) heterostructures (M = Ca, Sr), by means of Brillouin spectroscopy. The observed propagation of PSMs can be reasonably accounted for in terms of the simple theory of elasticity. Nevertheless, a lowering of 3–7% of the velocity values of the PSMs is detected in the case of leaky modes with relatively strong leakage. The observed deviations of the velocity of the PSMs are then thought to be connected with the presence of a region of roughness of the fluoride/GaAs(111) interface extending for several nanometres.

1. Introduction

For a detailed description of the effective acoustic properties of real solid systems with overlayers it is very important to find correlations between their structural characteristics and the velocities, attenuation factors, and surface acoustic mode spectral content. From this point of view epitaxial systems are favourable objects for investigation. In many practical cases their structural distortions are not very significant and experimentally detected surface acoustic wave data can be clearly interpreted in terms of simple elastic continuum theory [1]. On the other hand, in the case of CaF_2/Si(111) heterostructures the experimentally determined values of the Rayleigh mode (RM) velocity for several thicknesses (65, 100 nm [2] and 100–120 nm [3–5]) were found to be 3–5% lower than the calculated ones.

The lowering of RM velocity, V_{RM}, has been attributed to the presence of the so-called misfit dislocations [4, 5]. At early stages the growth of the CaF_2 film proceeds coherently, with the growing layer accurately following the planar parameter of the substrate. This produces a planar compression of the film. Thermal relaxation of mismatch stresses induces misfit defect formation, and the majority of these was found to be distributed in a region near the interface having a thickness that depends on the total thickness of the film, h [6]. For $h \simeq 100$ nm, the relative thickness of the distorted region appears to reach its maximum value (~ 30 nm). This leads to the detectable softening of the elastic properties of the structure and the corresponding 3–5% reduction of V_{RM}.

On the other hand, in the case of SrF_2/Si(111) heterostructures no systematic deviations between experimentally registered velocity V_{RM} values and calculated ones were found [5]. SrF_2/Si(111) is characterized by 6.8% lattice mismatch as compared to 0.6% lattice mismatch in the case of CaF_2/Si(111) heterostructures. A lattice mismatch of this size

0953-8984/94/183347+12$19.50

induces the presence of misfit dislocations right from the initial monolayer growth stage. These dislocations are highly concentrated in a thin interface region several nanometres thick [5], and its contribution to the total film thickness is negligible. In this case no lowering of the V_{RM} value was detected.

In other words, the different behaviour of the V_{RM} and consequently of the elastic properties of MF_2/Si(111) heterostructures, for M = Ca, Sr, can be explained by the existence of different scales of the thickness of the distorted region near the interface thickness, the probing sound wavelength being about 300 nm.

At $h \geqslant 150$–200 nm MF_2/Si(111) systems exhibited the presence of localized acoustic modes of Sezawa type [2, 4, 5]. Their velocities correlate with the calculated ones, but the deviations in the velocity were larger than those found for the RM. The latter may be connected with deeper oscillation of the higher-order modes into the substrate, and therefore a more pronounced influence of the defects of the region near the interface on the localized propagation of acoustic modes [2].

From this point of view, and due to its structure, the most sensitive modes to the presence of the defects in the interface region should be leaky, or so-called pseudo-surface modes (PSMs). In this case, and in contrast to the normal surface modes, only two of the three partial waves are evanescent when leaving the surface, whereas the third partial wave is an increasing one [8]. It is also important to notice that in MF_2/Si(111) systems the PSM was detected irregularly [2, 4] and this complicates its propagation studies.

Heterostructures of MF_2/GaAs(111) type (M = Ca, Sr) are proved to be a more suitable object for the investigation of how the presence of the interface defects would influence the PSM propagation. PSMs have been detected successfully in the substrate material, in a wide range of azimuthal directions close to $[1\bar{1}0]$ [9, 10]. Additionally, the existence of the PSM in a sufficiently wide range of the h parameter was predicted by theoretical calculation.

One may also stress that in contrast to MF_2/Si(111), the MF_2/GaAs(111) heterostructures are layered systems of 'accelerating' character. This means that the velocity of the RM increases with thickness until it reaches the V_{T_3} value (V_{T_3} is the velocity of a slow bulk transverse wave of the substrate having the same propagation direction as the RM), and then a degradation of the RM takes place, its energy being redistributed among collective surface excitations of the bulk velocity range $V > V_{T_3}$ [1, 11].

Additionally, the heterostructures with M = Ca, Sr have different relative layer/substrate velocity scales, thus allowing us to vary the character of the dispersion dependences.

2. Materials, instruments, and methods

The MF_2/GaAs(111) films were deposited on GaAs(111) wafers by molecular epitaxy in a research chamber. The substrate temperature was 530–600 °C, and the fluoride deposition rate was 3–5 nm min^{-1}. The quality of the lattice, as well as its surface morphology, was properly monitored during the growth using high-energy electron diffraction techniques [12]. The fluoride layer thickness h was determined by using both ellipsometry data (for details see [13]), and by interferometric methods, the experimental error being negligible.

For the present work CaF_2/GaAs(111) structures with film thickness h = 10, 20, 40, 50, 100, 120, 150, 160, 170, 220 nm and SrF_2/GaAs(111) systems with film thickness h = 10, 20, 50, 150, 230 nm have been chosen.

Propagation of RMs and PSMs in MF_2/GaAs(111) systems was investigated by the Brillouin spectroscopy method [14]. The registrations of the spectra of the scattered light were conducted by means of the five-pass piezoscanned Fabry–Perot interferometer of Burleigh. In all the experiments the electric vector E of the incident beam was parallel to

the plane of the incident light. Backscattering geometry was used. For a detailed description of the observation conditions see [4, 15].

As an example, spectra of light scattered by the (111) free surface of GaAs, and by an SrF_2/GaAs(111) heterostructure with $h = 150$ nm, are presented in figures 1 and 2 respectively (see also [11]). Surface waves propagate along the $[1\bar{1}0]$ direction in the (111) plane. Here Brillouin frequency shifts are also represented in velocity units, V, $V = \delta f \lambda/(2\sin(\alpha))$, where λ is the wavelength of the initial laser beam, and α is the angle of incidence.

One can see that the spectrum in figure 1 contains an intense satellite corresponding to a Rayleigh mode located at $\delta f = 10.84$ GHz (3.22 km s^{-1}), and another one related to the PSM, located at $\delta f = 8.11$ GHz (2.41 km s^{-1}). On the other hand, only the spectral component corresponding to the PSM was detected in the case of the sample with $h = 150$ nm, $\delta f = 9.26$ GHz (2.75 km s^{-1}).

Two theoretical approaches were employed in the identification of the Brillouin satellites registered, and to determine the velocities and attenuation factors of the PSMs and RMs. Both of them are based on the elasticity theory and employ as input in their calculations the stiffness coefficients of the bulk materials [1, 16].

One of the methods follows the scheme of [1], while the second one is based on the surface Green function matching (SGFM) method [17], and it has been used previously by us in the interpretation of the Brillouin spectra of semi-infinite systems. The SGFM method was also extended to study heterostructures with cubic symmetry [18]. It allows one to obtain the RM modes as well defined peaks outside the bulk continuum and the PSMs as the mostly Lorentzian peak merged in the continuum density of states [17]. The frequency distribution of surface phonons responsible for the Brillouin light scattering spectral content (i.e. normal and tangential displacements [14]) is shown in the lower parts of figures 1 and 2. Normal excitations causing dynamic corrugation of the surface (ripple light scattering mechanism) are depicted by the dashed curves, and the tangential ones, manifesting themselves via dielectric tensor modulation (elasto-optic coupling) are shown by the dotted lines.

The experimental attenuation of the PSM was estimated from Brillouin satellite linewidths, special deconvolution procedures being applied [19]. Due to the fall of Brillouin scattering cross section for the majority of the samples, $h = 100$–300 nm, caused by the destructive interference between the light scattered by both film surfaces [20, 21], the intensity of the Brillouin lines corresponding to the RM and PSM was insufficient for absolute attenuation value calculations. Meanwhile, the spectral components of light relating to the PSM were found to be wide enough to make proper qualitative linewidth comparisons, similar to those conducted by us earlier in [22, 23].

The velocity values obtained by both theoretical procedures are always the same. For the PSM attenuation rate (imaginary part of the velocity) we employed the method described in [1].

3. Experimental results

The dependence of surface acoustic wave velocities on the normalized layer thickness, qh, for a CaF_2/GaAs(111) heterostructure is represented in figure 3. Here the wave vector of the RM q is parallel to the $[1\bar{1}0]$ crystallographic direction. The positions of the maxima of the observed Brillouin satellites corresponding to the RM are marked by circles, the ones corresponding to the PSM by squares. Solid curves are calculated results for V_{RM} as well as PSM velocities (V_{PSM}). Experimental velocity values located at $qh = 0$ correspond to free (111) GaAs surface measurements.

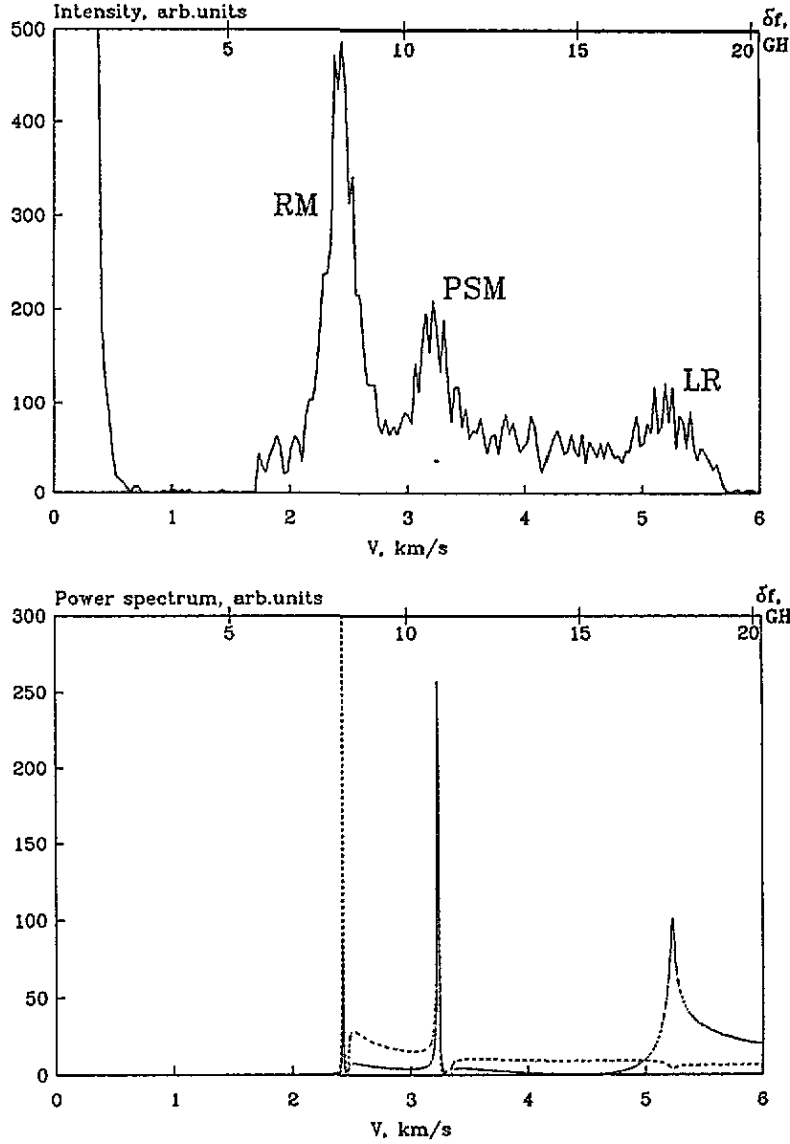

Figure 1. Brillouin spectrum of light scattered by a sample of GaAs with a (111) free surface. The surface wave vector q is parallel to the $[1\bar{1}0]$ direction, $\alpha = 60°$, $\lambda = 514.5$ nm. Brillouin lines corresponding to Rayleigh wave, pseudo-surface mode and longitudinal resonance are marked by RM, PSM and LR, respectively. The lower part of the figure represents the calculated surface phonon density distribution.

During Brillouin spectra registration the angle of incidence of the light, α, was varied from 40° to 70° for each sample investigated. This permits us to obtain several experimental values of the velocities of the RM an PSM corresponding to the region of $qh = (1.5\text{–}2.3)\times10^{-2}$ h. It should be remarked that the deviation between the experimental velocity values of the measurements of nearly equal qh parameters but for samples of different h do not exceed standard experimental error.

Figure 3 shows that a smooth increase of V_{RM} is observed with qh ranging from 0 to

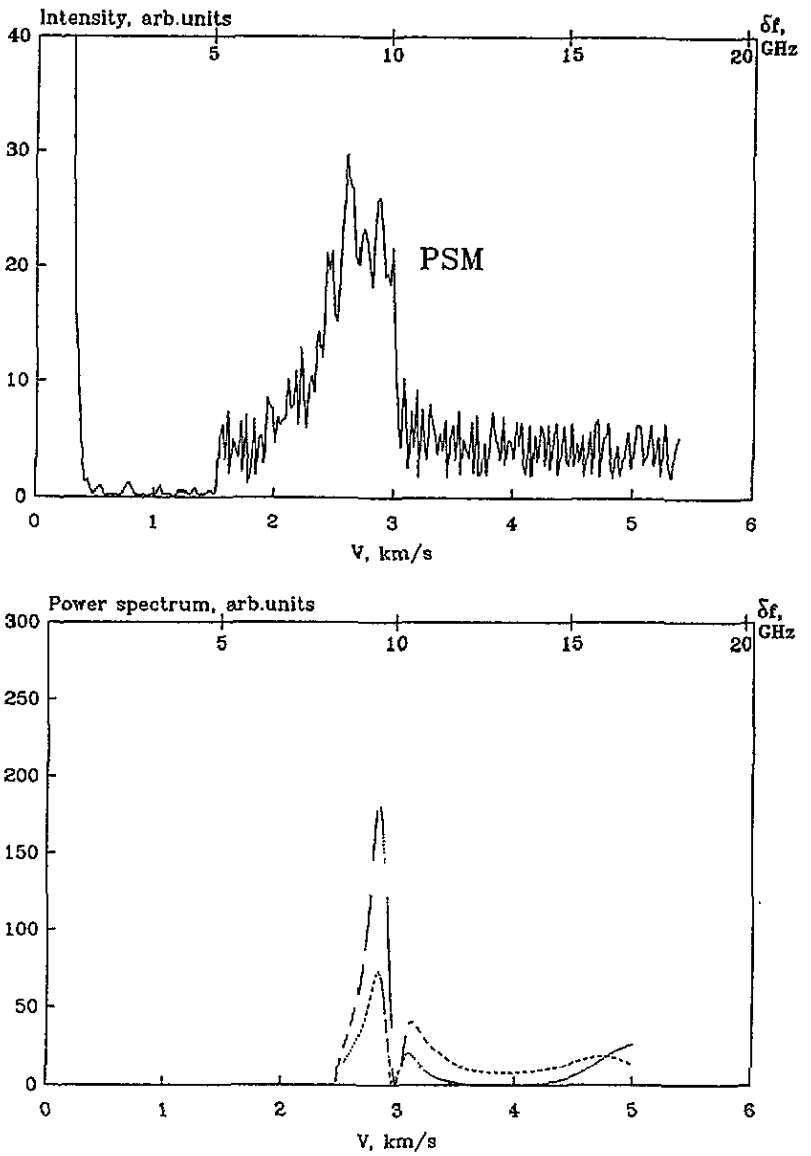

Figure 2. Brillouin spectrum of light scattered by an SrF_2/GaAs(111) heterostructure with $h = 150$ nm. The surface wave vector q is parallel to the $[1\bar{1}0]$ direction, $\alpha = 60°$, $\lambda = 514.5$ nm. Same conventions as in figure 1.

0.8, and the experimental velocity values are in good agreement with the calculated ones. In the range of $qh = 0.8$–1.2 the RM gradually degrades, and the corresponding Brillouin satellite was not detected [11].

In contrast with the RM degradation, the PSM exists in the whole span of qh. The PSM velocity is smoothly increased, reaching its maximum value, 3.295 km s^{-1}, at $qh \simeq 1.7$. Further qh increase leads to the V_{PSM} reduction asymptotically limited by the velocity of the layer material Rayleigh mode (see the broken horizontal line, $V = 3.18$ km s^{-1}). The experimental results for V_{PSM} appear to be correlated with calculated ones. Nevertheless,

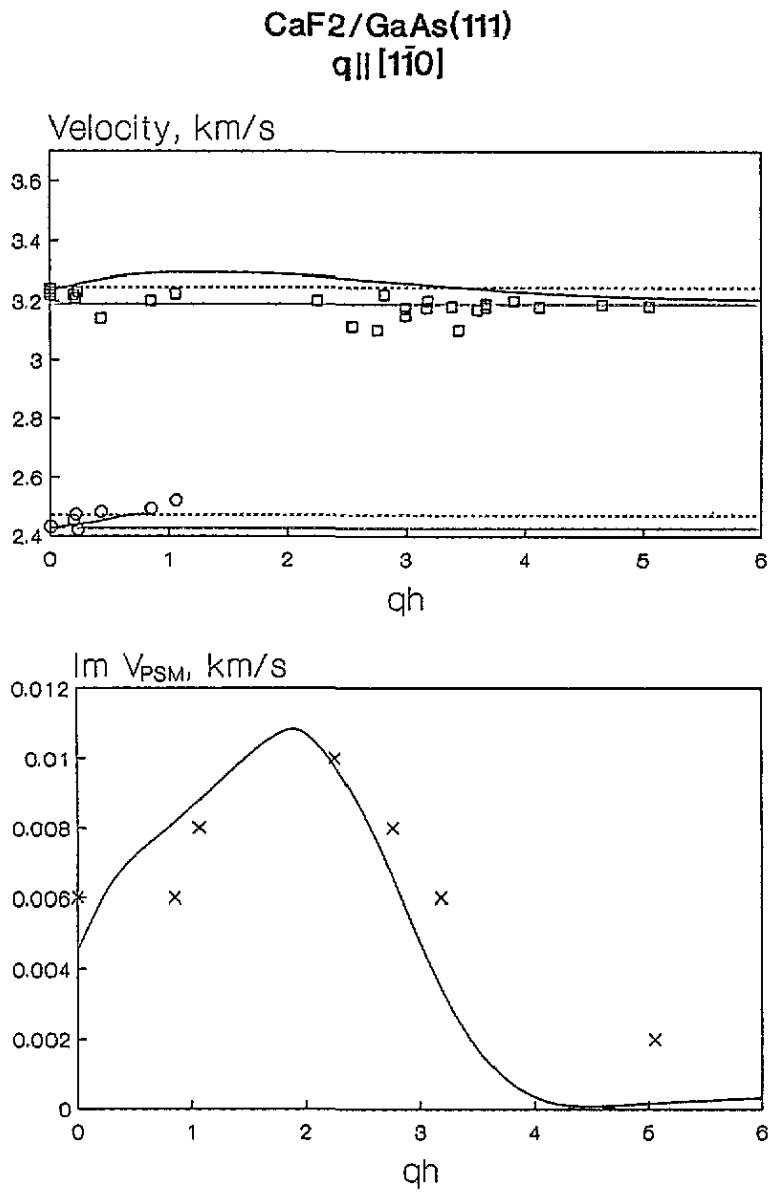

Figure 3. Experimental and calculated data for surface acoustic wave velocities versus qh in CaF_2/GaAs(111), $q \parallel [1\bar{1}0]$. Theoretical dispersion curves for the RM and PSM (solid lines) were calculated using elastic constants of bulk CaF_2 and GaAs [16]. Experimental velocity values are shown by circles; squares are those corresponding to the PSM. Broken horizontal lines mark the velocity values of the slow transverse bulk wave of the substrate material ($V_{T^s} = 2.47$ km s^{-1}), and the layer one ($V_{T^l} = 3.246$ km s^{-1}); $V_{RM^s} = 2.427$ km s^{-1}, corresponding to the RM velocity of the substrate material, and that of the layer, $V_{RM^l} = 3.19$ km s^{-1}, are represented by dotted curves. The lower part of the figure represents the calculated imaginary part of V_{PSM}, and the crosses are the results of the Brillouin satellite linewidth measurements expressed in arbitrary units.

one may observe that there is a 2–5% systematic deviation from corresponding theoretical

values toward lower-velocity ones.

The results of a calculation of the imaginary part of V_{PSM} are represented in the lower part of figure 3. Corresponding linewidths of Brillouin lines after deconvolution are shown on an arbitrary scale, and are represented by crosses. The linewidth value located at $qh = 0$ corresponds to the free (111) GaAs surface measurements.

One can observe qualitative agreement between the variation of the linewidth of the Brillouin satellite corresponding to the PSM and the character of the dotted curve describing PSM attenuation. It is seen from figure 3 that the PSM becomes the most rapid and the most 'leaky' at the same qh value, $qh \simeq 1.7$. With further qh increase the PSM attenuation decreases and by its structure the PSM is shown to go to the normal surface mode playing the role of the pre-Rayleigh mode of the system.

One may also conclude from figure 3 that the more leaky the PSM is, the greater the deviations from the calculated V_{PSM} values are. That is, V_{PSM} deviations reach 3–5% when PSM attenuation is maximal, $qh = 1$–3.5, but in the range of $qh < 1$, $qh > 3.5$, i.e. far from the maximum of the attenuation curve, V_{PSM} deviations do not exceed 2–2.5%.

The results of similar observations in the case of the SrF_2/GaAs(111) heterostructure are shown in figure 4. Here the RM velocity rises from 2.427 to 2.74 km s^{-1} with variation of qh, $qh = 0$–1.5, until finally the degradation of this mode takes place. In the whole area of RM existence good agreement between the experimental and calculated V_{RM} values can be observed.

With variation of qh from zero to six the V_{PSM} value is reduced monotonically from 3.2 to 2.67 km s^{-1}, and, as in the previous case, at large qh values the PSM is found to be a precursor of a new RM of the structure. Experimental values of V_{PSM} satisfactorily correlate with the theoretical curve, systematic deviations being practically absent for the regions of $qh = 0$–1, and for $qh \geqslant 4.5$. In the region of $qh = 1.5$–4 experimentally determined V_{PSM} values show a 4–7% lowering relative to the evaluated ones. Similarly to figure 3 the latter qh parameter values correspond to the maximal PSM attenuation (see the lower part of figure 4). The results of the determination of the satellite linewidth corresponding to the PSM are also represented. The variation of the linewidth versus qh agrees with the dotted curve, corresponding to the imaginary part of V_{PSM}.

For the $[1\bar{2}1]$ crystallographic direction, the velocities of the surface acoustic waves for different qh values are presented in figure 5 for CaF_2/GaAs(111) heterostructures. Note that for this propagation direction the particle displacements in the RM are found to be purely sagittal, and the PSM is initially ($qh = 0$) absent [8].

It is seen from figure 5 that with the increase of the qh parameter a degradation of the RM followed by a V_{RM} rise from 2.6 to 2.72 km s^{-1} is observed ($qh = 0$–1.5), and the measured V_{RM} values agree with the calculated ones. For the $qh = 1.5$–2.7 range the system does not show any reasonable surface resonance, and only at $qh = 2.7$–3 has a new surface excitation of typical layer material velocity values been formed [11].

This new excitation by its structure proves to be a PSM with a relatively strong attenuation at its initial stages, $qh = 3$–4. The velocity of the new mode monotonically decreases with increasing qh, asymptotically approaching the RM velocity limit of the layer material, and becoming less and less 'leaky'.

Values of the velocity of the new mode measured by Brillouin spectroscopy correlate with the theoretical curve, but deviate from it towards smaller velocities by 3–7%. As for the previous cases, the deviation appears to be more pronounced for the stronger attenuation values, $qh = 3$–4.

The results of surface acoustic wave velocity measurements in the SrF_2/GaAs(111) heterostructure for the $[1\bar{2}1]$ direction are shown in figure 6. Here, in contrast to figure 5,

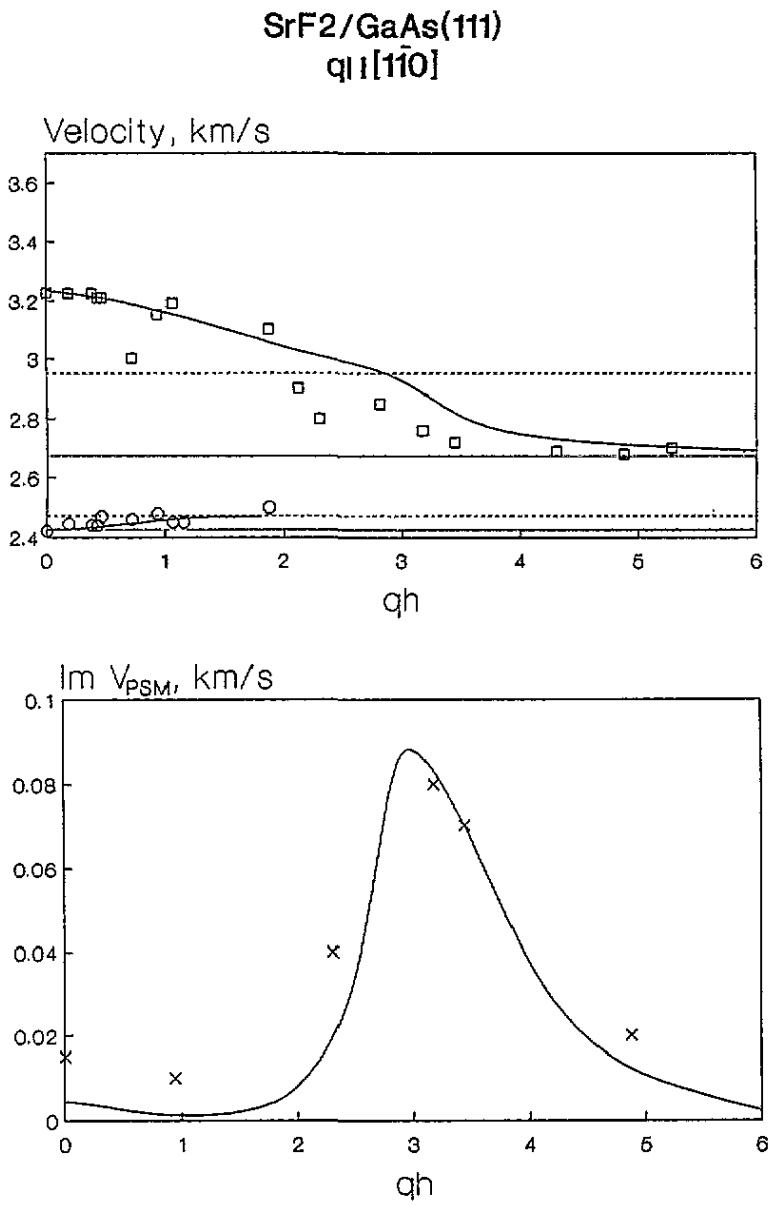

Figure 4. Experimental and calculated data for surface acoustic wave velocities versus qh in SrF_2/GaAs(111), $q \parallel [1\bar{1}0]$. Theoretical dispersion curves for RM, PSM were calculated using elastic constants of bulk SrF_2 and GaAs [16]. Same conventions as in figure 3. $V_{T^3} = 2.474$ km s^{-1}, $V_{T^1} = 2.95$ km s^{-1}; $V_{RM^3} = 2.427$ km s^{-1}, $V_{RM^1} = 2.675$ km s^{-1}.

the V_{T^3} value is found to be higher than the layer material Rayleigh velocity value—the 'upper' limit of V_{RM}. Therefore one should not expect the disappearance of the initial RM with qh increase, and the RM proves to be the normal mode of the structure in the whole span of qh. The latter is confirmed by a good coincidence between measured and calculated V_{RM} values, $qh = 0$–6.

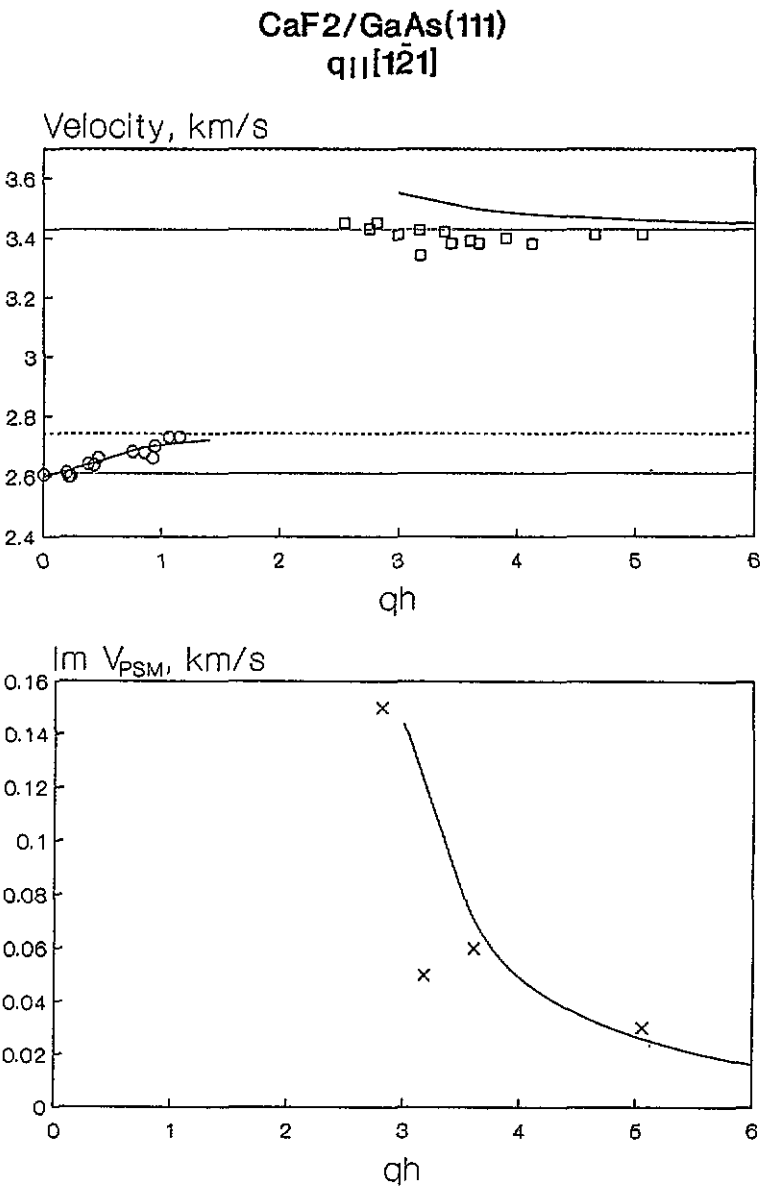

Figure 5. Experimental and calculated data for surface acoustic wave velocities versus qh in CaF_2/GaAs(111), $q \parallel [1\bar{2}1]$. Same conventions as in figure 3. $V_{T^3} = 2.749$ km s^{-1}, $V_{T^1} = 3.696$ km s^{-1}; $V_{RM^3} = 2.61$ km s^{-1}, $V_{RM^1} = 3.43$ km s^{-1}.

4. Discussion

Reasonable agreement between experimentally determined and calculated RM velocity values, as well as the ones of PSM characterized by relatively low leakage ($qh = 0$–1.5, > 4, figures 3, 4; $qh = 0$–1, > 5, figure 5) is observed for both MF_2/GaAs(111) structures, M = Ca, Sr. This fact shows their structural quality. Also, noticeable deviations of the measured V_{PSM} values from those predicted by the theory were detected for those qh regions where

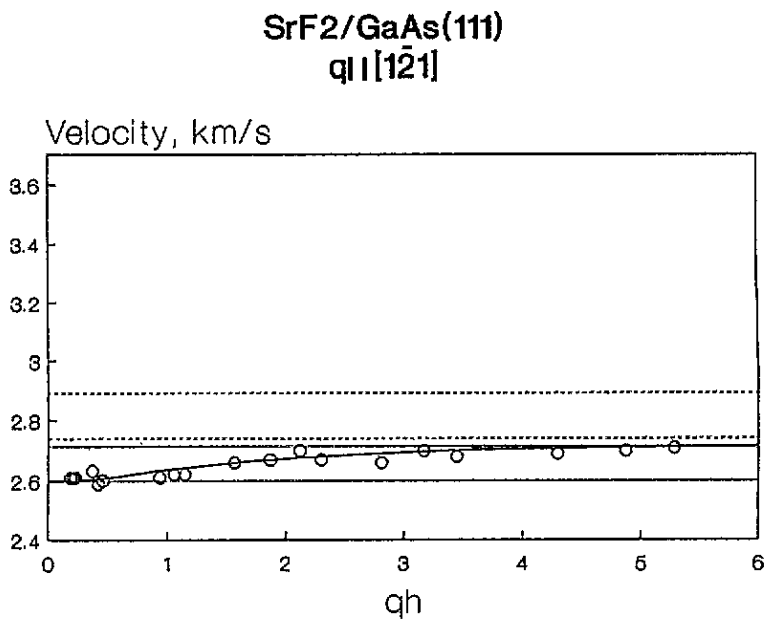

Figure 6. Experimental and calculated data for surface acoustic wave velocities versus qh in $SrF_2/GaAs(111)$, $q \parallel [1\bar{2}1]$. Same conventions as in figure 3. $V_{T^3} = 2.743$ km s^{-1}, $V_{T^1} = 2.893$ km s^{-1}; $V_{RM^3} = 2.6$ km s^{-1}, $V_{RM^1} = 2.717$ km s^{-1}.

the PSM leakage is relatively high: $qh = 1.5$–3, figure 3; $qh = 2$–4, figure 4; $qh = 3$–4, figure 5.

As in the case of the normal surface mode propagation we assume the observed deviation to be connected with structural properties of the region near the interface, depending here on the PSM attenuation magnitude. In fact, the attenuation of the leaky mode defines uniquely the degree of its wave vector deviation from surface into the bulk. The wave with stronger attenuation, i.e. with stronger deviation of its wave vector from the surface plane, must interact more deeply with the interface regions and so it probes deeper into the structure distortions than waves having a smaller attenuation or the normal modes.

In our opinion, the systematic 3–5% discrepancy in velocities in the case of PSM modes with a more pronounced attenuation, detected in both heterosystems, is connected with the interface roughness. After removing oxides from a GaAs wafer under As flux its (111) surface becomes rough, as was seen by 3D spots in the reflection high-energy diffraction pattern, the dimension of the hillocks being several nanometres [21]. During the fluoride film growth the surface becomes flatter, giving streaky diffraction patterns [22], but the buried interface roughness remains. It exists in all the films ($qh = 0$–6). However, it manifests itself in those structures, where the propagating modes are significantly leaky: $qh = 2.5$–3.5 figure 3; $qh = 1.5$–3 figure 5; $qh = 2$–4 figure 6.

The different sign of the lattice mismatch of $CaF_2/GaAs(111)$ and $SrF_2/GaAs(111)$ does not produce a difference in the elastic properties of the structures, because in both films misfit dislocations are strongly situated in the thin rough layer near the interface and give the same mechanism of thermal relaxation of stresses. This feature distinguishes $MF_2/GaAs(111)$ systems from the $MF_2/Si(111)$ structures studied earlier [2–5]. Atomic flatness of the Si substrate in the latter case gives rise to the divergence of the misfit stress relaxation among the two fluorides, and thus of the elastic properties of the structures.

Note that non-homogeneous defect distribution through the film depth in both types of heterostructure, MF_2/GaAs(111) and MF_2/Si(111), should lead to an equivalent variation of the local elastic properties of the layer versus h.

For 3–5% V_{RM} mismatch compensation in the case of CaF_2/Si(111) structures of $h \simeq 100$ nm where the region near the interface is 30 nm thick, the authors of [2] had to vary the elastic modulus values up to 10% in terms of the simple elastic continuum model.

This fact, as well as the results of our observations in MF_2/GaAs(111), shows that the local elastic properties of the fluoride/semiconductor heterostructures may considerably differ from those of the bulk material, and from continuum integrated estimations. Therefore, for the adequate characterization of the elastic properties of even fainter epitaxial systems theoretical models including flexible depth dependent elasticity variation should be developed. These models could be in the spirit of the planar defect approach [23], or the effective medium approximation [24], employed in the case of superlattices.

The behaviour of the Brillouin satellite linewidth corresponding to the PSM qualitatively follows the theoretical attenuation curve in all the cases discussed (see the lower parts of figures 3–5). However, present experimental spectral resolution was found to be insufficient to study the influence of the interface roughness on the PSM attenuation as well as on the broadening of the Brillouin satellites corresponding to RMs.

5. Conclusion

Both structures, MF_2/GaAs(111), M = Ca, Sr, exhibit the presence of Rayleigh and pseudo-surface acoustic waves, which are reasonably well described in terms of elastic continuum theory. The lowering of the experimentally detected V_{PSM} values is detected in the case of PSMs of relatively strong leakage. The observed V_{PSM} deviations are thought to be connected with the presence of a roughness of the fluoride/GaAs(111) interface region with a typical dimension of several nanometres.

Acknowledgment

The authors are very thankful to Professors N S Sokolov, A M Diakonov, and F García-Moliner for helpful discussions, and to Professor I A Yakovlev for his interest in our work. The contribution of VVA, and VRV was partially supported by NATO under Collaborative Research Grant No 930164.

References

[1] Farnell G W and Adler E L 1972 *Physical Acoustics* vol IX, ed W P Mason and R N Thurston (New York: Academic) p 35
[2] Karanikas J M, Sooryakumar R and Phillips J M 1989 *J. Appl. Phys.* **65** 3407
[3] Aleksandrov V V, Diakonov A M, Potapova Ju B and Sokolov N S 1992 *Pis. Zh. Tekh. Fiz.* **18** 44 (Engl. Transl. 1992 *Sov. Tech. Phys. Lett.* **18** 628)
[4] Aleksandrov V V, Potapova Ju B, Vorob'ev P A, Diakonov A M and Yakovlev N L 1993 *Sov. Phys.–Solid State* September issue
[5] Aleksandrov V V, Potapova Ju B, Diakonov A M and Yakovlev N L 1993 *Thin Solid Films* **234** at press
[6] Afanas'ev V V, Novikov S V, Sokolov N S and Yakovlev N L 1991 *Microelectron. Eng.* **15** 139
[7] Blunier S, Zogg H, Maiseu C, Tawari A N, Overney R H, Hoefke A and Kostorz G 1992 *Phys. Rev. Lett.* **68** 3599

[8] Farnell G W 1970 *Physical Acoustics* vol VI, ed W P Mason and R N Thurston (New York: Academic) p 109
[9] Carlotti G, Fioretto D, Giovannini D, Nizzoli F, Socino G and Verdini L 1992 *J. Phys.: Condens. Matter* **4** 257
[10] Aleksandrov V V, Velichkina T S, Potapova Ju B and Yakovlev I A 1992 *Zh. Eksp. Teor. Fiz.* **102** 1891 (Engl. Transl. 1992 *Sov. Phys.–JETP* **102** 1019)
[11] Detailed observations of the Rayleigh mode degradations conducted at CaF_2/GaAs(111) heterostructures are presented in
Aleksandrov V V, Bottani C E, Caglioti G, Ghislotti G, Marinoni C, Yakovlev N L and Sokolov N S 1994 to be published
[12] Gastev S V, Novikov S N, Sokolov N S and Yakovlev N L 1987 *Pis. Zh. Tech. Fiz.* **13** 961 (Engl. Transl. 1987 *Sov. Tech. Phys. Lett.* **13** 401)
[13] Holmes D A 1967 *Appl. Opt.* **6** 168
[14] Nizzoli F and Sandercock J R 1990 *Dynamical Properties of Solids* vol 6, ed H K Horton and A A Maradudin (Amsterdam: North-Holland) p 281
[15] Aleksandrov V V, Velichkina T S, Voronkova V I, Diakonov A M, Syrnikov P P, Yakovlev I A and Yanovskii V K 1989 *Phys. Lett.* **142A** 307
[16] *Landolt–Bornstein New Series* 1966, 1983 Group III, vol 1 (Berlin: Springer) p 17
[17] Velasco V R and García-Moliner F 1980 *J. Phys. C: Solid State Phys.* **13** 2237; 1980 *Solid State Commun.* **33** 1
García-Moliner F and Velasco V R 1992 *Theory of Single and Multiple Interfaces* (Singapore: World Scientific)
[18] Sanz-Velasco E, Hardouin Duparc O and Velasco V R 1983 *Surf. Sci.* **126** 202
Hardouin Duparc O and Velasco V R 1983 *Phys. Status Solidus* b **117** K37
Hardouin Duparc O, Sanz-Velasco E and Velasco V R 1984 *Phys. Rev.* B **30** 2042
[19] Lindsay S M, Burgess S and Shepherd I W 1977 *Appl. Opt.* **16** 1404
[20] Bortolani V, Marvin A M, Nizzoli F and Santoro G 1983 *J. Phys. C: Solid State Phys.* **16** 1757
[21] Karanikas J M, Sooryakumar R and Phillips J M 1989 *Phys. Rev.* B **39** 1388
[22] Aleksandrov V V, Velichkina T S, Potapova Ju B and Yakovlev I A 1992 *Phys. Lett.* **171A** 103
[23] Aleksandrov V V, Velichkina T S, Vorob'ev P G, Potapova Ju B and Yakovlev I A 1993 *Zh. Eksp. Teor. Fiz.* **103** 2170 (Engl. Transl. 1993 *Sov. Phys.–JETP* **76** 1085)
[24] Tsutsui K, Mizukami H, Ishiyama O, Nakamura S and Furukawa S 1990 *Japan. J. Appl. Phys.* **29** 468
[25] Schowalter L J and Fathauer R W 1986 *J. Vac. Sci. Technol.* A **4** 1026
[26] Kosevich A M and Khokhlov V I 1968 *Sov. Phys.–Solid State* **10** 39
Velasco V R and García-Moliner F 1979 *Phys. Scr.* **20** 111
Velasco V R and Djafari-Rouhani B 1982 *Phys. Rev.* B **26** 1929
[27] Grimsditch M and Nizzoli F 1986 *Phys. Rev.* B **33** 5821
Djafari-Rouhani B and Sapriel J 1986 *Phys. Rev.* B **34** 7114
Nougaoui A and Djafari-Rouhani B 1987 *Surf. Sci.* **185** 125